united nations
educational, scientific
and cultural
organization

international atomic
energy agency

the
abdus salam
international centre for theoretical physics

SMR/1157 - 21

SCHOOL ON
NEURAL INFORMATION PROCESSING

3 - 28 May 1999

SYNAPTIC DYNAMICS

Misha TSODYKS
Department of Neurobiology
Weizmann Institute of Science
Rehovot 76100
Israel

Lecture 1: Information transmission through depressing synapses.

Misha Tsodyks

May 20, 1999

Department of Neurobiology, Weizmann Institute of Science, Rehovot 76100, Israel.

1 Summary

It is well known that transmission of spike trains across neocortical synapses depends on the history of presynaptic activity (see [Thomson and Deuchars, 1994] for a recent review). Majority of the synapses, connecting pyramidal cells, exhibit fast synaptic depression of the response. This property can be accurately captured by a simple kinetic model which describes the release of the neurotransmitter cause by the presynaptic spike. The model predicted that the amplitude of the postsynaptic potential is inversely proportional to the frequency of presynaptic spikes above a certain limiting frequency. This prediction was confirmed experimentally. This special property results in saturation of spatially summated postsynaptic responses from a population of presynaptic neurons, preventing signaling of their firing rates. However, at the moments of synchronized transitions in firing rates within the presynaptic population, a novel set of postsynaptic signals emerge, expressed as transient postsynaptic currents. Temporal redistribution of synaptic efficacy [Markram and Tsodyks, 1996] changes the limiting frequency as well as the transient signals.

2 Experimental background

A marked feature of synaptic contacts between neocortical pyramidal neurons is fast synaptic depression (FSD) of the postsynaptic responses during a train of presynaptic spikes [Thomson and Deuchars, 1994]. For a periodic train at a particular frequency, the responses depress steadily until they reach the frequency-dependent steady level (Fig. 1). Experiments showed [Tsodyks and Markram, 1997, Abbott et al., 1997] that the steady amplitude of the excitatory postsynaptic potential (EPSP) decreases inversely proportional to the action potential (AP) frequency above a certain limit (defined as the limiting frequency, Fig. 1A,B). Thus for the lower firing rates, the product of EPSP amplitude and presynaptic frequency and hence the time-averaged postsynaptic membrane potential, increases gradually with frequency, while for higher firing rates the postsynaptic response remains almost constant (Fig. 1C, observed). This synaptic behavior is strikingly different from the behavior which would be exhibited in the absence of depression, in which case the postsynaptic membrane potential would grow linearly with the presynaptic frequency (Fig. 1C, linear case). Neocortical neurons receive synaptic input from large populations of presynaptic neurons, in which case spatial summation at each moment may replace the temporal averaging performed above for an individual connection. The question then arises what signal can be transmitted to a pyramidal neuron from a population of other pyramidal neurons. Furthermore, long-term synaptic plasticity induced by simultaneous activation of pre- and post-synaptic neurons was reflected in a change in the rate of synaptic depression, or in temporal redistribution of synaptic efficacy (RSE) over consecutive spikes in a train [Markram and Tsodyks, 1996]. This result raises the question of how RSE effects interpyramidal signaling.

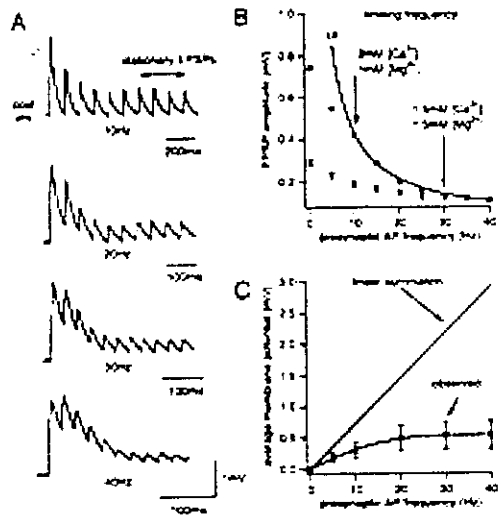

Figure 1: Frequency dependent synaptic depression; (A) EPSPs generated by presynaptic spike trains at various frequencies (average of 20 sweeps). (B) Stationary EPSPs. Solid line shows inverse relationship with frequency. Limiting frequency is defined as the frequency above which the EPSP amplitude is $\propto 1/f$. (C) Time-averaged membrane potential in postsynaptic neurons relative to resting potential as a function of presynaptic AP frequency ($n = 7$; observed). Straight line - linear summation.

3 Phenomenological model of depressing synapses

We address these issues with an integrated approach based on experiments as well as a functional model of interpyramidal synapses [Tsodyks and Markram, 1997]. The model is analogous to a three-state kinetic scheme for receptor desensitization [Destexhe et al., 1994]. In this scheme, influx of the neurotransmitter into the synaptic cleft opens some fraction of receptors, which then desensitize with a time constant of a few milliseconds and recover with a time constant of about 1 second. Alternatively, one could think of a presynaptic mechanism of depression, in which a neurotransmitter released by an action potential is slowly replenished in order to be used by subsequent spikes. Both of these mechanisms lead to the same mathematical formulation. For concreteness, we will adopt the presynaptic mechanism:

$$\begin{aligned} \frac{dx}{dt} &= \frac{z}{\tau_{rec}} - Ux(tsp - eps)\delta(t - tsp) \\ \frac{dy}{dt} &= -\frac{y}{\tau_{rel}} + Ux(tsp - eps)\delta(t - tsp) \\ z &= 1 - x - y, \end{aligned} \tag{1}$$

where x, y, z are the fraction of neurotransmitter in the recovered, active (released) and inactive states correspondingly; U is a parameter which determines the fraction of the recovered neurotransmitter released by each presynaptic spike; τ_{in} $sim1msec$ and $\tau_{rec} \sim 1sec$ are the time constants of neurotransmitter inactivation and recovery, respectively. The net postsynaptic current is proportional to the fraction of neurotransmitter in the active state:

$$I_{post} = Ay(t), \tag{2}$$

where the constant A is called an *absolute* strength of the synapse, which equals the maximal response which could be emitted if all of the neurotrasnmitter would be emitted ($y = 1$). Here we neglect trial by trial fluctuations in the synaptic responses, including failures since synaptic input from large populations of neurons are expected to average out these fluctuations.

The model equations 1 can be further simplified if one assumes that the time interval between subsequent spikes is much larger then τ_{in}. In this case $y << 1$ for most of the time and one can derive iterative expressions for successive amplitudes of excitatory postsynaptic currents (EPSCs) produced by a train of presynaptic spikes:

$$EPSC_{n+1} = EPSC_n(1 - U)e^{-\Delta t/\tau_{rec}} + AU(1 - e^{-\Delta t/\tau_{rec}}), \tag{3}$$

where $EPSC_n$ is the amplitude of the postsynaptic current for nth ($n = 0, 1, 2...$) spike in a train, and Δt is the time interval between nth and $(n + 1)$th spike, which is assumed to be larger than the time constant of receptor desensitization. One should note that parameters A and U play complementary roles; A defines the absolute synaptic strength, determined by the overall amount of receptors, while U determines the distribution of synaptic strength over consecutive spikes (for example, reflecting the probability of release [Stevens and Wang, 1994]). This model captures the essential synaptic behavior for both regular and irregular spike trains (Fig. 2B,C), but does not necessarily reflect the biophysical mechanism of FSD, which is not known.

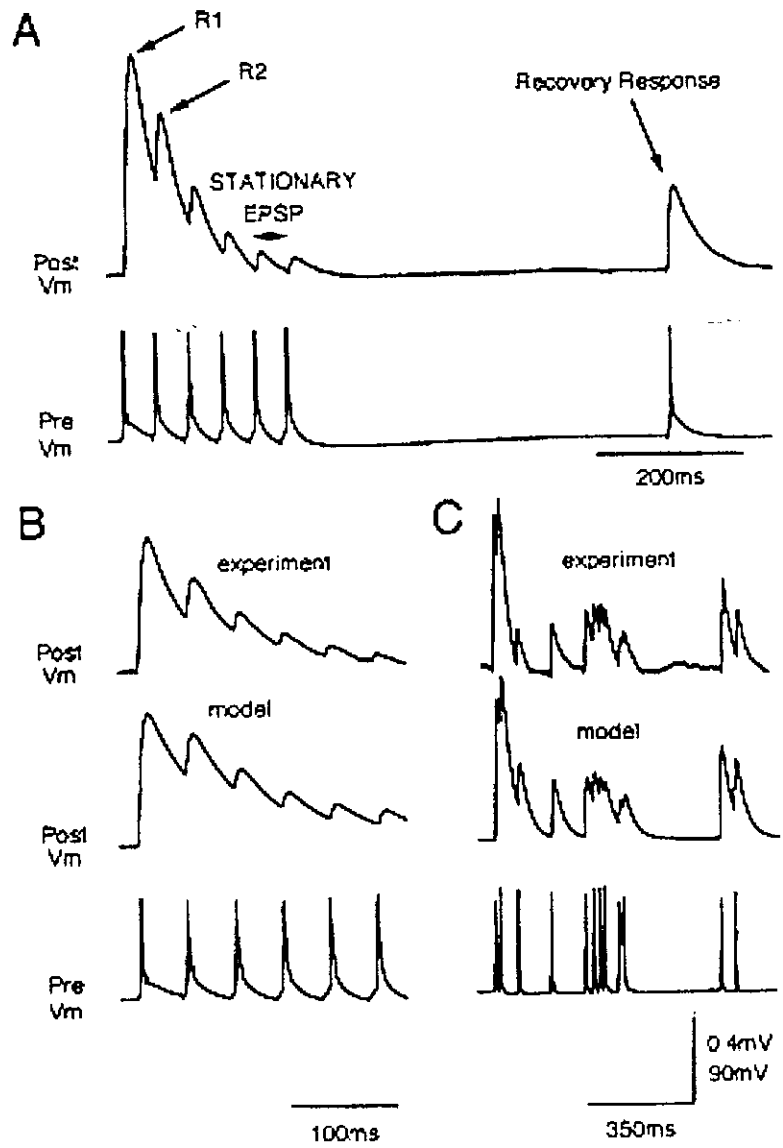

Figure 2: Functional synaptic model. (A) Stimulation paradigm used to obtain the parameters for the model. (B) Postsynaptic potential generated by a regular spike train (lower-most trace) at a frequency of 23 Hz measured experimentally (top trace; average more than 50 sweeps) and computed with the model (middle trace). (C) Same as in B for irregular spike train (different synapse).

4 Transmission of firing rates via depressing synapses

To test whether the model can simulate the special properties of FSD and RSE, lets consider the stationary level of $EPSC$s ($EPSC_{st}$) reached during a regular spike train, which equals

$$EPSC_{st} \approx A\frac{\Delta t}{\tau_{rec}} = \frac{A}{f\tau_{rec}}, \tag{4}$$

provided the frequency of presynaptic spikes is high enough ($f >> \frac{1}{U\tau_{rec}}$). This result is consistent with the experimental observation (Fig. 1B) that EPSP amplitude is inversely proportional to presynaptic AP frequency. The level of $EPSC_{st}$ in this region of frequencies does not depend on U. An increase in U therefore results in a *conditional* potentiation only at lower frequencies, while an increase in A results in an *unconditional* potentiation at any frequency. RSE did not change stationary synaptic responses for high frequencies (Fig. 3A) [Markram and Tsodyks, 1996] and therefore did not alter A. Indeed, changing only the distribution parameter effectively simulates RSE (Fig. 3B), as well as effects of neuromodulators (Fig. 3E).

To estimate frequency dependent signaling between neocortical pyramidal neurons under *in vivo* conditions [Softky and Koch, 1993] we computed the stationary postsynaptic currents generated by a large population of n presynaptic neurons firing Poisson spike trains with the rate r:

$$I_{post} = An\frac{r\tau_{in}d}{1 + rU\tau_{rec})}. \tag{5}$$

The frequency dependence of I_{post} is determined by parameters U and τ_{rec}. The possible range of behaviors derived from the statistics of experimentally examined synapses is shown

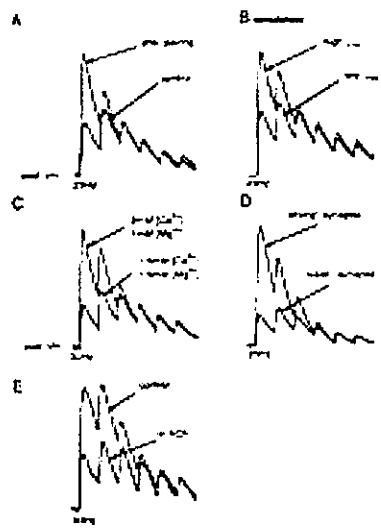

Figure 3: Changing the amount of synaptic utilization by APs: (A) Effect of pairing pre and postsynaptic APs on the synaptic response to a 23 Hz train of presynaptic APs (experiment). (B) Changing U can mimic the effect of pairing. $U = 0.35$ before pairing, $U = 0.67$ after pairing. (C) Lowering extracellular calcium slows the rate of synaptic depression. (D) Two different synaptic connections selected to demonstrate that while the initial responses (low frequency) were markedly different the stationary EPSPs (high frequency) were the same. (E) Redistribution of synaptic efficacy caused by acetylcholine (ACh).

in Figure 4A. To test the accuracy of these predictions, we computed the analogous time-averaged membrane potential for Poisson spike trains for a single neuron. Indeed, we found that the time-averaged membrane potentials recorded experimentally when the presynaptic neuron was forced to generate Poisson spike trains (see methods) at different rates and the predicted behavior matched (Fig. 4B,C).

5 Transmission of synchrony via depressing synapses

We then looked into the postsynaptic current which results after *synchronized* changes in firing rates within the population. An entirely novel set of signals in a postsynaptic neuron was observed in simulations (Fig. 5). These signals emerge due to spatial summation of responses originating from multiple neurons involved in the transition and are expressed as *transient* postsynaptic currents which have characteristic amplitude, shape and duration depending on the nature of the transition and the distribution parameter of synapses. The traces B1 and B2 illustrate the different properties of synaptic transmission with different values of U, indicating the functional significance of RSE . Higher values of U resulted in more pronounced current transients for low *initial* frequencies without significantly changing the baseline (compare 1st and 2nd transitions). Neocortical neurons can be reliably driven by sharp current transients [Mainen and Sejnowski, 1995], suggesting that a postsynaptic neuron could encode these rate transitions in its AP output. We therefore injected the computed current into pyramidal neurons (Fig. 5, upper traces). The AP responses to the same presynaptic population activity after RSE were fundamentally different in that AP responses after RSE (higher U) reflected exclusively presynaptic rate transitions, while the

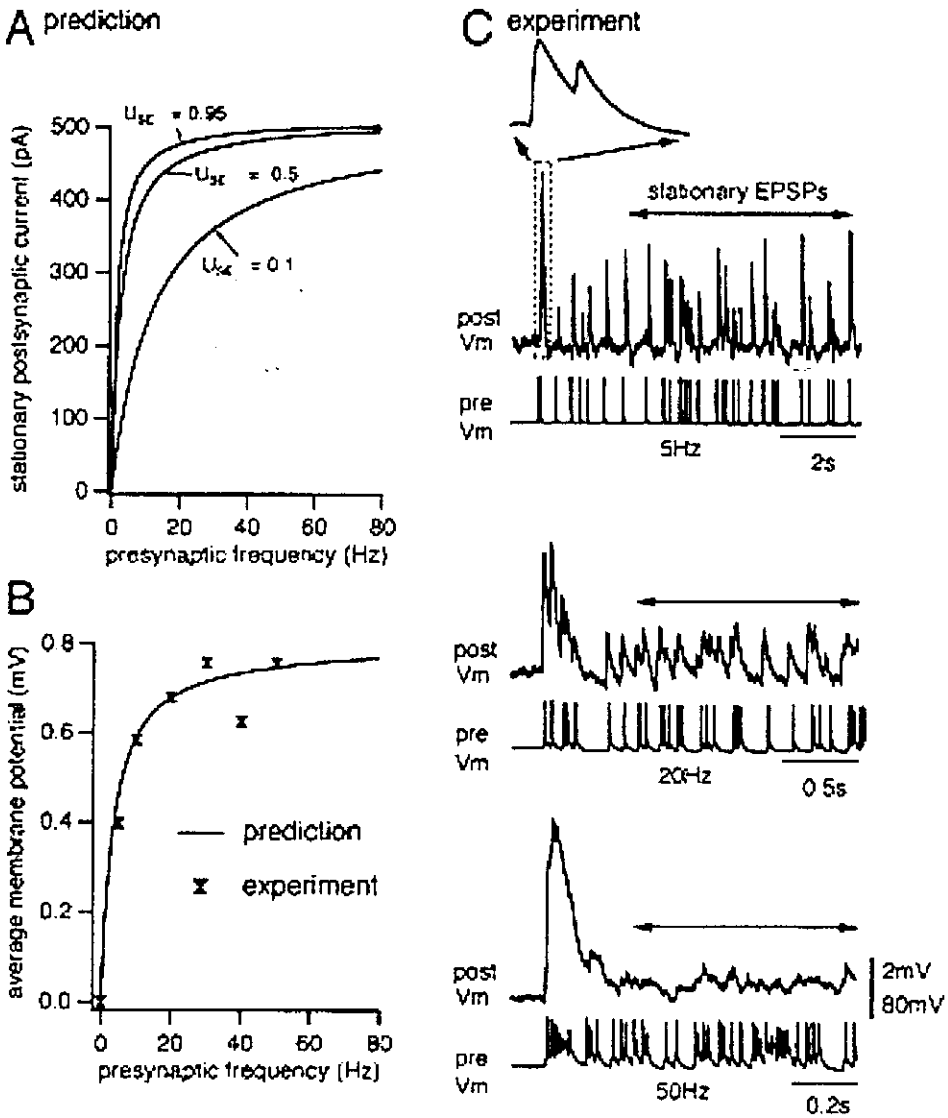

Figure 4: (A) The computed spatially summated synaptic input from n = 500 presynaptic neurons firing Poisson trains as a function of their firing rates r. (B) Computed time-averaged membrane potential at different presynaptic spiking frequencies. Superimposed are the experimental time-averaged membrane potentials from the neuron represented in C. (C) Experimentally recorded EPSPs generated by Poisson presynaptic spike trains at various frequencies. Arrows indicate the time window over which the time-averaged membrane potentials shown in B were determined.

responses before RSE were more sustained and largely reflected the sustained rate of the presynaptic population.

6 Conclusion

The analysis demonstrated that (1) interpyramidal synapses have a natural range of limiting frequencies for rate signaling, dictated by the novel features of fast synaptic depression, (2) RSE constitutes a means to change these limiting frequencies, (3) RSE is *conditional* potentiation and should be distinguished from *unconditional* synaptic potentiation, (4) novel signals are generated when presynaptic populations change gear and (5) RSE modulates these novel signals.

References

[Abbott et al., 1997] Abbott, L. F., Varela, J. A., Sen, K., and Nelson, S. B. (1997). Synaptic depression and cortical gain control. *Science*, 275:220–224.

[Abeles, 1991] Abeles, M. (1991). *Corticonics*. Cambridge University Press, New York.

[Destexhe et al., 1994] Destexhe, A., Mainene, Z. F., and Sejnowski, T. J. (1994). Synthesis of models for excitable membranes, synaptic transmission and neuromodulation using a common kinetic formalism. *J. Comp. Neurosci.*, 1:195–230.

[Mainen and Sejnowski, 1995] Mainen, Z. F. and Sejnowski, T. J. (1995). Reliability of spike timing in neocortical neurons. *Science*, 268:1503–1506.

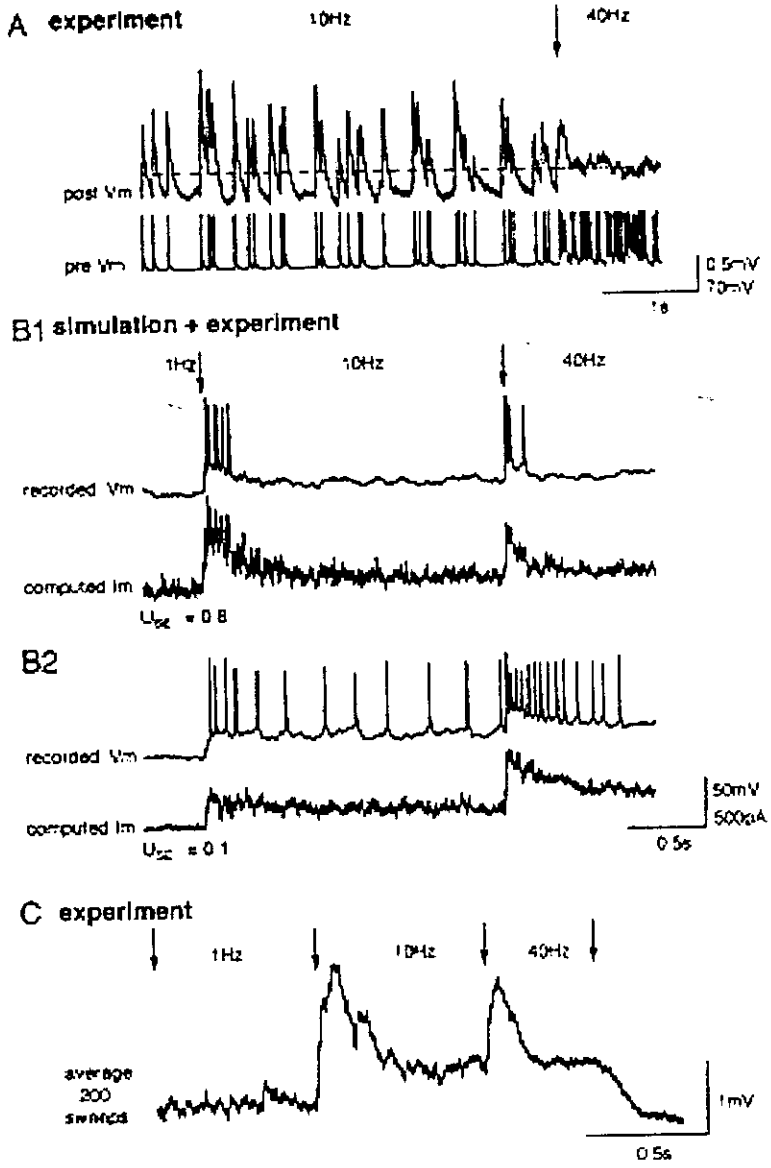

Figure 5: Signaling of synchronized transitions in the activity of a population of presynaptic neurons. (A) Experimentally recorded EPSPs generated by a Poisson spike train undergoing transition (indicated by arrow) from 10 Hz to 40 Hz. The average membrane potentials before and after the transition were equal. (B1) The simulated postsynaptic current, generated by Poisson spike trains of a population of 500 presynaptic neurons with synchronous transitions from 1 Hz to 10 Hz and then to 40 Hz, together with the response of a pyramidal neuron when the simulated synaptic current was injected into the soma. (B2) The same as B1 but with lower value of U. (C) Average voltage response recorded from a postsynaptic neuron after stimulating the presynaptic neuron with the sequence of 200 *different* Poisson spike trains undergoing the same transitions as in B.

[Markram and Tsodyks, 1996] Markram, H. and Tsodyks, M. V. (1996). Redistribution of synaptic efficacy between pyramidal neurons. *Nature*, 382:807–810.

[Softky and Koch, 1993] Softky, W. R. and Koch, C. (1993). The higly irregular firing of cortical cells isinconsistent with temporal integration of random EPSPs. *J. Neurosci.*, 13:334–350.

[Stevens and Wang, 1994] Stevens, C. F. and Wang, Y. (1994). Changes in reliability of synaptic function as a mechanism for plasticity. *Nature*, 371:704–707.

[Thomson and Deuchars, 1994] Thomson, A. M. and Deuchars, J. (1994). Temporal and spatial properties of local circuits in neocortex. *Trends Neurosci.*, 17:119–126.

[Tsodyks and Markram, 1997] Tsodyks, M. and Markram, H. (1997). The neural code between neocortical pyramidal neurons depends on neurotransmitter release probability. *PNAS*, 94:719–723.

Lecture 2: Differential Signaling via the Same Axon from Neocortical Pyramidal Neurons

Misha Tsodyks

May 20, 1999

Department of Neurobiology, Weizmann Institute of Science, Rehovot 76100, Israel.

1 Summary

Neural information encoded within action potentials may be transmitted to hundreds of target neurons. Simultaneous whole-cell recordings from 3-4 neurons in neocortical slices revealed that synaptic responses evoked by trains of action potentials from a single pyramidal neuron and transmitted by the same axon could exhibit different dynamics for each target neuron. A homogeneous class of pyramidal targets responded to action potential activity with different maximal responses, rates of activity dependent synaptic depression and recovery from depression. Interneurons innervated with the same axon responded in an entirely opposite manner with powerful activity dependent synaptic *facilitation*. The computational significance of differential signaling onto pyramidal and interneurons was examined and we found that it enables pyramidal neurons to recruit variable proportions of excitation and inhibition depending on the characteristics of the action potential activity in the presynaptic pyramidal neurons. Differential signaling via the same axon suggests that any single action potential or any given train of action potentials has a unique significance for each target neuron in the context of network activity and could therefore be fundamental to how the neocortex decifers the neuron code.

2 Introduction and experimental background

Our approach to understanding the neural code is to determine how the properties of synaptic transmission dictate what features of the action potential train are effectively transmitted to postsynaptic neurons. We showed in the previous lecture that the rate of depression of synaptic responses, which is typical for synapses between pyramidal neurons, determines whether synapses are suitable to transmit information about the temporal synchrony in a presynaptic population, the average rate or a combination of the two (Tsodyks and Markram, 1997; Abbott et al., 1997). We also showed that Hebbian pairing causes a change in the rate of synaptic depression and hence serves to modulate the spike train features that the synapses are most suitable to transmit.

In order to understand how the nervous system decifers the code within an action potential train it would therefore be necessary to determine the properties of synaptic transmission at every one of the several thousand possible outputs of the axonal tree. While this is not yet feasible, one could attempt to determine how the synaptic response produced by the same axon innervating two neurons of a homogeneous class or two neurons of different classes compared.

We first examined synaptic transmission onto two layer 5 pyramidal neurons. Of 9 triple cell recordings in which all the cells were coupled, 4 were examples of divergent innervation from one neuron onto two (Fig.1). Anatomical reconstructions used to determine the location of putative light-microscopically identified synaptic contacts revealed that the same axon can form synapses on different parts of the dendritic tree of two neurons that are morphologically indistinguishable (Markram et al., 1998) which could form the basis for different processing of the same presynaptic signal in the two neurons(Fig. 1A,B). Those connections which produced physiologically detectable responses in the soma were different in the three features analyzed, absolute synaptic strength (A) which is a parameter that describes the maximum potential synaptic response that could be produced by an action potential, the U parameter which describes the average fraction of A that an action potential utilizes and a time constant for recovery from depression (t_{rec}). These results show that connections onto a homogeneous class of neuron can be anatomically and physiologically different.

While connections onto neurons of the same class where quantitatively different, those onto interneurons were qualitatively different. In particular while the synaptic response onto pyramidal neurons displayed the characteristic activity dependent synaptic depression the connection onto interneurons displayed remarkable activity dependent synaptic facilitation that could readily build up to discharge the neuron (Fig.2). In this lecture we will focus on the computational significance of such different synaptic responses.

3 Model

We extend the model used for depressing synapses to include the facilitating effects. A standard way of modeling short term facilitation is by introducing a 'facilitation factor' which is elevated by each spike by a certain amount and decays between spikes, possibly at several rates. To add facilitation into our synaptic model, we therefore assume that the value of U (see the previous lecture) is not fixed but increased by a certain amount due to each presynaptic spike. The resulting model includes both facilitating and depressing mechanisms:

$$\begin{aligned} \frac{dx}{dt} &= \frac{z}{\tau_{rec}} - ux\delta(t-t_{sp}) \\ \frac{dy}{dt} &= -\frac{y}{\tau_{in}} + ux\delta(t-t_{sp}) \\ \frac{dz}{dt} &= \frac{y}{\tau_{in}} - \frac{z}{\tau_{rec}} \end{aligned} \tag{1}$$

All the variables in these equations have the same meaning as in the corresponding equations of the previous lecture, except that u now stands for the *running* value of the utilization parameter. The corresponding kinetic equation for this variable reads:

$$\frac{du}{dt} = -\frac{u}{\tau_{facil}} + U(1-u)\delta(t-t_{sp}). \tag{2}$$

U is a parameter which determines the increase in the value of u due to each spike and coincides with the value of u reached upon the arrival of the first spike (in other words, at very low frequency of stimulation).

This equation can be transformed into an iterative expression for the value of u reached upon the arrival of n-th spike in a train, which determines the post-synaptic response according to Eqs. 1:

$$u(n+1) = u(n)(1-U)exp(-\delta t/\tau_{facil}) + U \tag{3}$$

where δt is the time interval between the n-th and $(n+1)$-th spikes. If the presynaptic neuron emits a regular spike train at the frequency r, u reaches a steady value of

$$\frac{U}{1-(1-U)exp(-1/r\tau_{facil})}.$$

Thus in this formulation, u is a frequency dependent variable and U is a kinetic parameter characterizing an activity dependent transmission in a given synapse.

4 Differential synaptic transmission onto pyramidal neurons and interneurons

We should emphasize that facilitating and depressing mechanisms are intricately interconnected since stronger facilitation leads to higher u values which in turn leads to stronger depression. The value of U together with a new time constant τ_{facil} determine the contribution of facilitation in generating subsequent synaptic responses. We found that the main features of synaptic transmission between pyramidal neurons and inhibitory inter-neurons are well captured by this model with $U \sim 0.01 \rightarrow 0.05$ and τ_{rec} is typically several times faster than τ_{facil} (Markram et al., 1998). Depressing synapses on the other hand are characterized by higher U values and very short (if any) τ_{facil}.

5 Frequency dependence of facilitating synaptic connections

When facilitating synapses are stimulated at progressively higher frequencies, the steady-state amplitude of EPSPs for a given frequency (termed EPSPst) first increases and then decreases resulting in a bell-shaped curve (Fig. 3D). This behavior differs from the frequency dependence of depressing synapses, where EPSPst decrease as the frequency increases

(Tsodyks and Markram, 1997), due to simultaneous facilitation of u and growing depression at higher values of u (see Eq. 2). The peak of the bell-shaped curve is a characteristic feature of a particular facilitating synapse and can be derived from the model equations by finding the frequency where the product of the steady-state values of u and R are at a maximum. An approximate expression for this characteristic frequency (which we called 'peak frequency') is

$$\theta = 1/\tau_{facil} + \sqrt{2/\tau_{facil}^2 + \frac{1+U}{U\tau_{rec}\tau_{facil}}} \approx 1/\sqrt{U\tau_{rec}\tau_{facil}}, \quad (4)$$

The dependency of a peak frequency on the model parameters can be used to approximate this characteristic frequency for any facilitating synapse.

Another characteristic property, previously found for depressing synapses, which also applies to facilitating synapses, is the limiting frequency (λ). The limiting frequency is the frequency of stimulation where EPSPst begin to decrease inversely proportional to the frequency (Fig. 4B). λ is a characteristic property of synapses because it reflects a specific relationship between U and recovery from depression and, if present, facilitation. λ typically ranges from 5-30 Hz for depressing synaptic connections (Tsodyks and Markram, 1997). λ values for facilitating synapses are considerably higher (70-130 Hz).

6 Transmission of rates and synchrony via facilitating synapses

The model was used to examine which features of presynaptic APs are transmitted to the postsynaptic neuron. The frequency dependence of EPSPst illustrated in Fig. 4B indicates that the transmission properties of neocortical synapses are very different depending on the rate of presynaptic AP discharge. When the net steady-state postsynaptic membrane potential was plotted against the presynaptic frequency, a sigmoidal relationship was revealed that points to three frequency regimes defined as supra-linear, linear, and sub-linear signaling regimes (Fig. 4C). Fig. 4D illustrates a particular example of responses generated by instantaneous frequency transitions. These traces reveal that, in the sub-linear regime (at rates near and above λ), the steady-state response is insensitive to the presynaptic frequency because of synaptic depression, as is the case with depressing synapses. More precisely, the product of EPSPst and frequency saturates. The main feature that is transmitted to the postsynaptic neuron in this signaling regime is changes in frequencies (see Fig. 4D, sub).

The linear signaling regime begins below λ, where the postsynaptic response reflects a progressively higher contribution of the absolute discharge rate of the presynaptic neuron as the frequency decreases toward . Near θ, the postsynaptic response is proportional to the discharge rate (see Fig. 4D, linear). Both the sub-linear and linear signaling regimes exist as well for depressing synapses (Tsodyks and Markram, 1997), but their linear regime is in a narrow range of low frequencies.

The novel supra-linear regime for facilitating synapses begins below θ and extends toward 0 Hz. In this regime, the postsynaptic response can be approximated by multiplying the

discharge rate with the number of APs emitted during the preceding time window of facil (see Fig. 4D, supra) (Markram et al., 1998).

This analysis demonstrate that the values of θ and λ , which are dependent on the values of the synaptic parameters $U, t_{rec}, , t_{facil}$, determine the frequency ranges within which the basic signaling regimes exist and hence underlie the transmission properties of synapses.

7 Conclusion

In conclusion, we described differential synaptic signaling in the neocortex. The innervation of a homogeneous class of neurons can be anatomically and physiologically different, but the dynamics of synaptic transmission are qualitatively the same. On the other hand, the innervation of two different types of neurons can result in nearly opposite dynamics. Revealing the different biophysical properties of these two distinct types of synapses and the manner in which the presynaptic terminal is transformed when a specific type of neuron is contacted would be of utmost importance in order to isolate the governing principles behind differential synaptic transmission of potentially thousands of synapses that are formed by the axonal tree. Pyramidal neurons may contact other types of interneurons and pyramidal neurons each with a characteristic range of synaptic properties, potentially making each population uniquely sensitive to specific characteristics of the activity patterns within the pyramidal population. Dynamic synapses may therefore indeed enable a sophisticated mechanism of feature extraction. It also seems that any view of how information is encoded within the action potential train can not overlook the view from the synapses.

8 Figure Legends

Figure 1. Examples of synaptic responses onto two pyramidal neurons from a single presynaptic pyramidal neuron.

Figure 2. Differential synaptic facilitation and depression via the same axon innervating two different targets - pyramidal cell and interneuron. Single trial responses (30 Hz) to the same action potential train.

Figure 3 Phenomenological synaptic model. (A) Simulated post-synaptic potential generated by a regular spike train at a frequency of 20 Hz transmitted through a depressing synapse. (B) Same as in A for facilitating synapse. (C) Same as B but for a presynaptic frequency of 70 Hz. (D) Stationary level of EPSPs vs presynaptic frequency for facilitating synapses. Open circles - experimental results for one of the recorded synaptic connections between pyramidal neuron and inhibitory interneuron; solid line - model results.

The post-synaptic potential is computed using a passive membrane mechanism ($\tau_{mem}\frac{dV}{dt} = -V + R_{in}I_{syn}(t)$) with an input resistance of $R_{in} = 100M\Omega$ for pyramidal target and $1Giga\Omega$ for interneuron. Parameters: (A): $\tau_{mem} = 40$ msec; $\tau_{inact} = 3$ msec; $A = 250$ pA; $\tau_{rec} = 800$ msec; $U = 0.5$; (BCD) $\tau_{mem} = 60$ msec; $\tau_{inact} = 1.5$ msec; $A = 1540$ pA; $\tau_{rec} = 130$ msec; $\tau_{facil} = 530$ msec; $U = 0.03$;

Figure 4

Frequency dependence, signaling regimes, and synaptic transfer functions of facilitating synapses. (A1) Average EPSPs (4 sweeps) recorded in interneuron (30 Hz). (A2) Simulated synaptic response (30 Hz). Postsynaptic potential is computed by using a passive membrane mechanism $t_{mem}dV/dt = V + (RinIsyn(t))$ with Rin of 1 G and $t_{mem} = 60ms$ (V = voltage, Isyn = synaptic current). (B) Steady-state EPSP amplitudes vs. presynaptic AP frequency. Each point represents average of 20-30 EPSPst. Solid line, model calculation. Same synaptic connection as in A. Dashed line, inverse relationship with frequency. Peak frequency marked as θ, limiting frequency as λ is determined when the model fit of the experimental data deviates 10depolarization as a function of presynaptic frequency (product of EPSPst, presynaptic frequency and membrane time constant, 60 ms). (D) Simulated postsynaptic current (Im) generated by Poisson AP trains with a sequence of instantaneous transitions from 0 to 80 Hz. Model parameters, $A = 1,540pA, U = 0.03, t_{rec} = 130ms, t_{facil} = 530ms$. The trace represents the average of 500 "sweeps."

References

Abbott, L. F., Varela, J. A., Sen, K., and Nelson, S. B. (1997). Synaptic depression and cortical gain control. *Science*, 275:220–224.

Markram, H., Wang, Y., and Tsodyks, M. (1998). Differential signaling via the same axon from neocortical layer 5 pyramidal neurons. *PNAS*, 95:5323–5328.

Tsodyks, M. and Markram, H. (1997). The neural code between neocortical pyramidal neurons depends on neurotransmitter release probability. *PNAS*, 94:719–723.

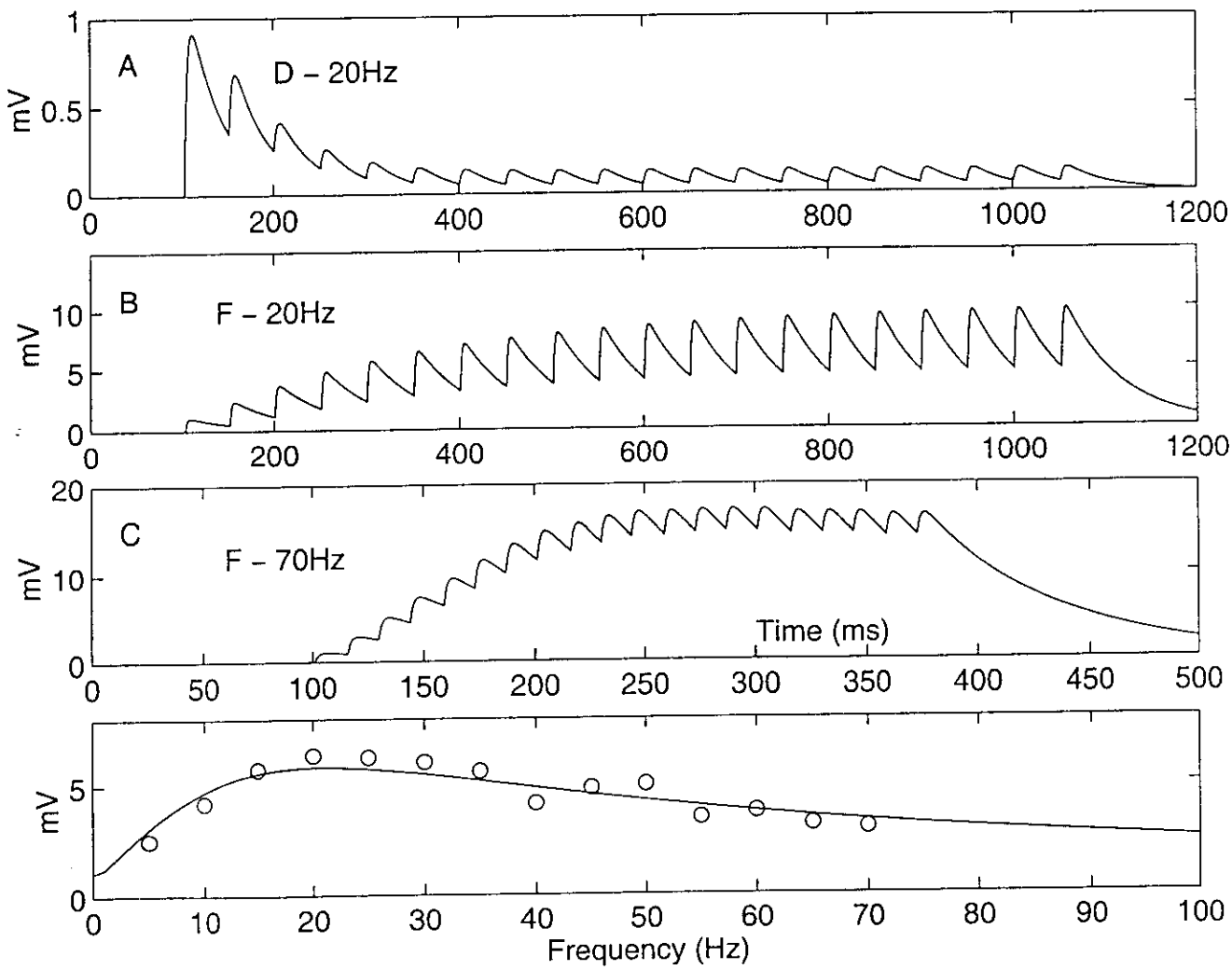
A
D – 20Hz
mV
1
0.5
0
0
200
400
600
800
1000
1200
B
F – 20Hz
mV
10
5
0
0
200
400
600
800
1000
1200
C
F – 70Hz
mV
20
10
0
Time (ms)
0
50
100
150
200
250
300
350
400
450
500
mV
5
0
0
10
20
30
40
50
60
70
80
90
100
Frequency (Hz)

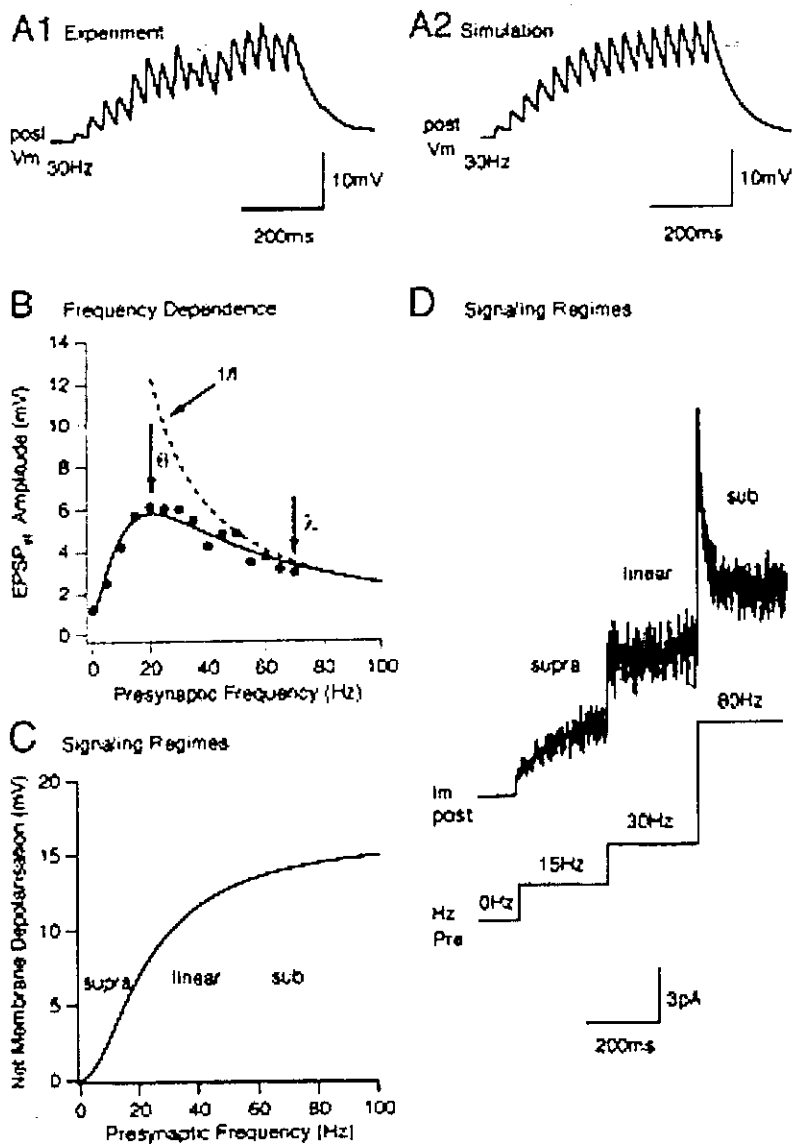
A1 Experiment
post
Vm
30Hz
10mV
200ms
A2 Simulation
post
Vm
30Hz
10mV
200ms
B Frequency Dependence
EPSP Amplitude (mV)
1/f
Presynapoc Frequency (Hz)
C Signaling Regimes
Net Membrane Depolarisation (mV)
supra
linear
sub
Presynaptic Frequency (Hz)
D Signaling Regimes
sub
linear
supra
80Hz
Im
post
30Hz
15Hz
0Hz
Hz
Pre
3pA
200ms

Lecture 3: Neural Networks with Dynamic Synapses - Mean-Field

Misha Tsodyks

May 20, 1999

Department of Neurobiology, Weizmann Institute of Science, Rehovot 76100, Israel

1 Summary

Here we describe how can the unified phenomenological model of dynamic synapses be used in order to analyze the dynamics of large interconnected neural networks. We derive mean0field equation which govern the evolution of the activity of different subpopulations in the network. We show that dynamics of synaptic transmission results in complex sets of regular and irregular regimes of network activity.

2 Introduction

As we showed in the previous lectures, the nature of dynamic synaptic transmission transmission varies between different classes of neurons. The phenomenological formulation of depressing synapses between pyramidal neurons was generalized to describe facilitating synapses between pyramidal cells and inhibitory interneurons. This formulation has two major goals. First, it allows the quantification of the features of the AP activity of the

presynaptic neurons and populations transmitted by these different types of synapses. Second, it can be used in deriving a novel mean-field dynamics of neocortical networks aimed at understanding the dynamic behavior of large neuronal populations without having to solve an equally large number of equations. Mean-field descriptions were extensively used in order to understand the possible computations of cortical neural networks (see e.g. Wilson & Cowan 1972, Amit & Tsodyks 1991, Ginsburg & Sompolinsky 1994, Tsodyks *et al* 1997). The novel formulation which uses the generalized phenomenological model of dynamic properties of synaptic connections between different types of neocortical neurons allows to study the effects of synaptic dynamics and synaptic plasticity on information processing in large neural networks.

3 Derivation of the mean-field equations.

In order to derive a coarse-grained description of neuronal dynamics we have to compute the post-synaptic current generated by a population of neurons with a particular firing rate. This can be done using the phenomenological model of dynamic synapses introduced in the previous lectures:

$$\begin{aligned} \frac{dx}{dt} &= \frac{z}{\tau_{rec}} - ux\delta(t-t_{sp}) \\ \frac{dy}{dt} &= -\frac{y}{\tau_{in}} + ux\delta(t-t_{sp}) \\ \frac{dz}{dt} &= \frac{y}{\tau_{in}} - \frac{z}{\tau_{rec}} \end{aligned} \tag{1}$$

where x, y and z are the fractions of resources in the recovered, active and inactive states respectively. The post-synaptic current is taken to be proportional to the fraction of resources in the active state, $I_s(t) = Ay(t)$ where A is the absolute synaptic strength which can only be exhibited by activating all of the resources.

Facilitation effects are included as an increase in the value of u due to each pre-synaptic spike. The resulting model therefore includes both facilitating and depressing mechanisms. The corresponding kinetic equation reads:

$$\frac{u}{dt} = -\frac{u}{\tau_{facil}} + U(1-u)\delta(t-t_{sp}). \tag{2}$$

U determines the increase in the value of u due to each spike and coincides with the value of u reached upon the arrival of the first spike (in other words, at very low frequency of stimulation).

We now go back to our original problem of signaling from a large population of presynaptic neurons. There is an infinite number of ways the neurons of a population can fire relative to each other. Analysis of neurophysiological data revealed that individual neurons *in-vivo* fire irregularly at all rates (Softky & Koch 1993), reminiscent of the so-called Poisson process. Mathematically, the Poisson assumption means that at each moment the probability for a neuron to fire is given by the value of the instantaneous firing rate and is independent of the timing of previous spikes. This assumption allows averaging the equations 1, 2 over different realizations of Poisson trains with a given rate, to obtain the new dynamics for the corresponding mean quantities (Amit & Tsodyks 1991):

$$\begin{aligned}
\frac{d<x>}{dt} &= \frac{1-<x>}{\tau_{rec}} - <u><x>r(t) \\
\frac{d<u^->}{dt} &= -\frac{<u^->}{\tau_{facil}} + U(1-<u^->)r(t) \\
<u> &= <U_{SE}^->(1-U_{SE}) + U_{SE}
\end{aligned} \tag{3}$$

where $r(t)$ denotes the rate of a Poisson train for the neuron at time t. $< u^- >$ denotes the average value of u immediately before the spike. Depressing synapses are described by the first of these equations with the fixed value of u. In deriving Eqs. 3 we made a further simplification by assuming that the inactivation time constant τ_{in} is much faster than the recovery one τ_{rec}. This assumption is valid for inter-pyramidal synapses studied in (Markram & Tsodyks 1996) and for pyramidal - inter-neuron synapses (Markram *et al*, 1998). The evolution of post-synaptic current can be obtained from the remaining equation for y and recalling that $I_s(t) = Ay(t)$:

$$\frac{d<y>}{dt} = -\frac{<y>}{\tau_{in}} + <u><x>r(t). \tag{4}$$

which can be simplified to $y = r\tau_{in}u < x >$ if one is interested only in the time scale slower than τ_{in}.

We should mention that while averaging equations 1 over different realizations of Poisson spike trains, we assumed that there is no statistical dependence between the variables $x(t)$ and $u(t)$ and the probability of spike emission at time t. This is strictly valid only if there is no facilitation since in this case u is a fixed parameter of the model and $x(t)$, which is a function of the spike arrival times prior to the current time, is independent of the probability of a spike at time t due to the Poisson assumption. However, if facilitation is included, both

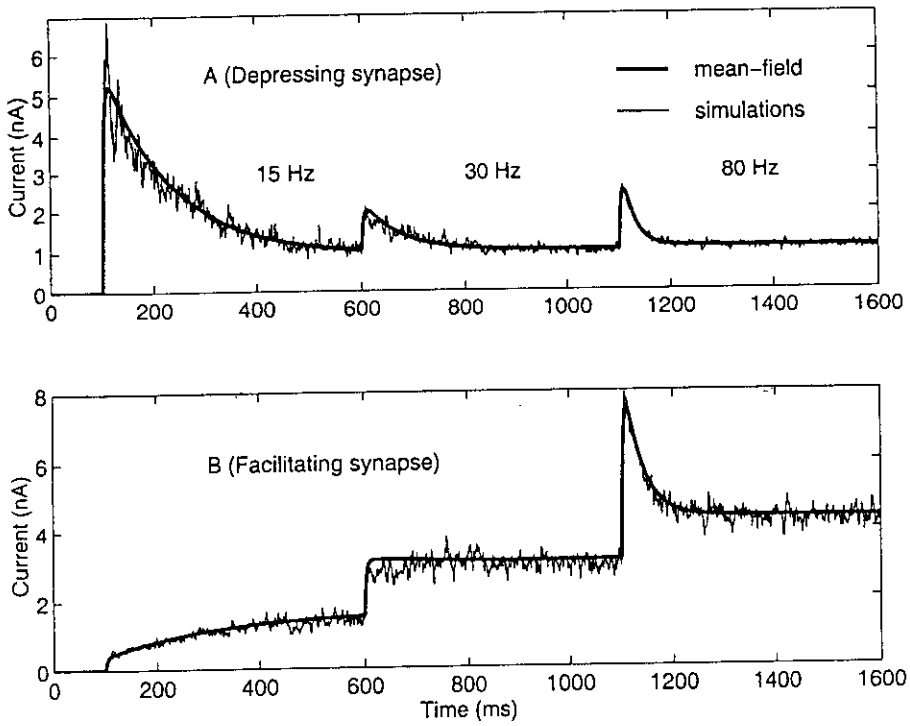

Figure 1: Post-synaptic current, generated by Poisson spike trains of a population of 1000 neurons with synchronous transitions from 0 Hz to 15 Hz to 30 Hz and then to 80 Hz, transmitted through facilitating (A) and depressing (B) synapses. Thick line - solution of mean-field equations 4, 5; thin line - simulations of 1000 spike trains with the use of the full model (Eqs. 1, 2).

$x(t)$ and $u(t)$ are a function of previous spikes and are thus not statistically independent. We thus performed simulations of equations 1, 2 for populations of presynaptic neurons firing Poisson spike trains with various modulations of their firing rate and compared the resulting post-synaptic current with the solution of the mean-field equations 3. We found that in all cases considered, mean-field solutions were good approximations (Fig. 1).

Equations 3, 4 can be solved analytically for an arbitrary modulation of the firing rates of the presynaptic population. In the case of depressing synapses, the solution takes a particular

simple form:

$$< y(t) >= Ur(t) \int_{-\infty}^{t} dt' exp(-\frac{t-t'}{\tau_{rec}} - \int_{t'}^{t} dt'' Ur(t'')) \quad (5)$$

We use this equation to determine which features of the presynaptic AP train are transmitted by depressing synapses to their targets. Assuming that the presynaptic frequency changes gradually, one can write down the expansion over the derivatives of the frequency. The first two terms of this expansion are

$$\frac{r}{1+rU\tau_{rec}} + r' \frac{r}{(1+rU\tau_{rec})^3} + ... \quad (6)$$

This expression describes the relative contribution of rate and temporal signaling in generating the postsynaptic response. The first term depends on the current rate which is dominant for frequencies which are small compared to the *limiting* frequency $\lambda \sim 1/(U\tau_{rec})$. As the frequency increases this term saturates and thus progressively less rate signaling is possible. The main contribution at higher frequencies therefore comes from a transient term reflecting the changes in frequencies. In the context of population signaling, this means that only synchronous transitions in the population activity can be signaled to the postsynaptic neuron (Tsodyks & Markram 1997).

The solution of the full set of equations 3 for facilitating synapse has the same form as Eq. 6 with the single complication due to the fact that u is now a functional of the frequency

$$u = U \int_{-\infty}^{t} dt' r(t') exp(-\frac{t-t'}{\tau_{facil}} - U \int_{t'}^{t} dt'' r(t'')) \quad (7)$$

which has to be substituted in the Eq. 6. One could still analyze the qualitative features of

this solution by noting that at very high frequencies, $u \to 1$ and thus facilitating synapses behave in the same way as depressing ones, transmitting the information about the rate transitions. As the frequency decreases towards the 'peak frequency' (see Lecture 2)

$$\theta = 1/\tau_{facil} + \sqrt{2/\tau_{facil}^2 + \frac{1+U}{U\tau_{rec}\tau_{facil}}} \approx 1/\sqrt{U\tau_{rec}\tau_{facil}}, \tag{8}$$

the presynaptic rate dominates in the postsynaptic response. The reason for this is that at this frequency facilitating and depressing effects compensate each other and the average amplitude of EPSP, which is $\sim xu$, is approximately constant. At even smaller frequencies depressing effects become less relevant since x recovers to almost unity between the subsequent spikes. In this regime the postsynaptic signal mainly reflects the current value of rate amplified by the value of u:

$$I_s \sim r(t) \int_{-\infty}^{t} dt' r(t') exp(-(t-t')/\tau_{facil}) \tag{9}$$

The integral in this equation is roughly equal to the number of spikes emitted by the presynaptic neuron in the preceding time window of τ_{facil}. In this regime, postsynaptic response is a delayed and amplified transformation of the presynaptic frequency.

As an example, we show in Fig. 1 the post-synaptic current resulting from a series of transitions in the firing rate for both depressing and facilitating synapses. All three regimes of transmission via facilitating synapses are illustrated in Fig. 1B.

4 Mean field network dynamics

The analysis of the previous section allows the formulation of a closed system of equations for the dynamics of a large network consisting of subpopulations of neurons with uniform connections. Each population could describe a cortical column which consists of neurons with similar receptive field properties. We assume that at each cortical location there are only two subpopulations of cortical neurons, comprised of pyramidal excitatory neurons and inhibitory inter-neurons. The coarse grained equations, describing the firing rates of these populations, have the same form as in (Wilson & Cowan 1972, Amit & Tsodyks 1991):

$$\begin{aligned} \tau_e \frac{dE_r}{dt} &= -E_r + g(\sum_{r'} J^{ee}_{rr'} y^{ee}_{r'} - J^{ei}_{rr'} y^{ei}_{rr'} + I^e_r) \\ \tau_i \frac{dI_r}{dt} &= -I_r + g(\sum_{r'} J^{ie}_{rr'} y^{ie}_{r'} - J^{ii}_{rr'} y^{ii}_{rr'} + I^i_r), \end{aligned} \tag{10}$$

where E_r (I_r) is the firing rate of excitatory (inhibitory) populations located at the site r; g(x) is a response function usually assumed to be monotonously increasing; $J^{ee}_{rr'}$ denotes the absolute strength of the synaptic connection between excitatory neurons in the populations located at r and r' times the average number of such connections per one post-synaptic neuron, correspondingly for other interactions. Finally, I^e_r (I^i_r) is the external input to the excitatory (inhibitory) population. $y^{ee}_{rr'}$ (and corresponding values for all other synapses) has to be computed from the equations 3, 4 for each connection rr' with the corresponding set of kinetic parameters. Refractoriness of the neurons was ignored for simplicity.

These equations reduce to the ones of Wilson and Cowan (1972) if synaptic transmission is frequency independent, in which case $x_r \equiv 1$ and hence $y_r \sim E_r$. In the presence of frequency

dependence they include effects of ever-changing synaptic efficacy due to depression and facilitation.

4.1 Network of one population

As the most simple example we consider a network which consists of only one population of excitatory neurons. Already in this case synaptic depression makes the network dynamics nontrivial. Equations 10 reduce to

$$\begin{aligned} \tau \frac{dE}{dt} &= -E(t) + g(JUx(t)E(t)) \\ \frac{dx}{dt} &= -UE(t)x(t) + \frac{1 - x(t)}{\tau_{rec}} \end{aligned} \tag{11}$$

For convenience, the factor of τ_{in} (see Eq. 4) was absorbed in the definition of J. One can solve these equations for the fixed point, where it simplifies into

$$E = g(JU \frac{E}{1 + EU\tau_{rec}}) \tag{12}$$

and can be illustrated using the graphical method (Fig. 2A). The rhs of Eq. 12 always saturates for arbitrary response functions due to synaptic depression. The system will therefore have a nontrivial fixed point with $E > 0$ even in cases where without depression there is no stable solution.

The stability of the fixed point solution can be analyzed from Eqs. 11. The solution is stable if the following matrix has eigenvalues with negative real parts:

$$\begin{pmatrix} \frac{\beta JUx^*-1}{\tau} & \frac{\beta JUE^*}{\tau} \\ -Ux^* & -UE^* - \frac{1}{\tau_{rec}} \end{pmatrix} \tag{13}$$

where E^* and x^* are the values of E and x at the fixed point, $\beta = g'(JUx^*E^*)$. For a linear-threshold gain function ($\beta = const$) as in Fig. 2A, the phase diagram of the system is shown in Fig. 2B. For a given threshold, a fixed point solution appears when the synaptic strength exceeds the first critical value shown by the lower line on the diagram. Contrary to what one would expect from Fig. 2A, this solution remains unstable until the synaptic strength grows above a second critical value (upper line).

Even if the fixed point solution is stable, the system exhibits damped oscillations before reaching the steady state due to synaptic dynamics (Fig. 2C).

4.2 Network of two interconnected populations

This system was analyzed in (Wilson & Cowan 1972) for the case of linear synapses. They showed that if the external inputs are fixed, mean-field equations have two basic types of stable solutions - fixed points and limit cycles with the period on the order of τ_e, τ_i. In the present case, the mean-field equations have a much richer set of solutions because in addition to the pair of equations for E and I (Eq. 10) they also include dynamic equations for synaptic efficacies (Eq. 3). As a result, in addition to fixed points and simple limit cycles, the system exhibits a variety of rhythmic and irregular solutions which dominate the network behavior but are difficult to analyze in a completely general manner. Two particular novel solutions, one periodic and another irregular, are shown in Fig. 3A, B.

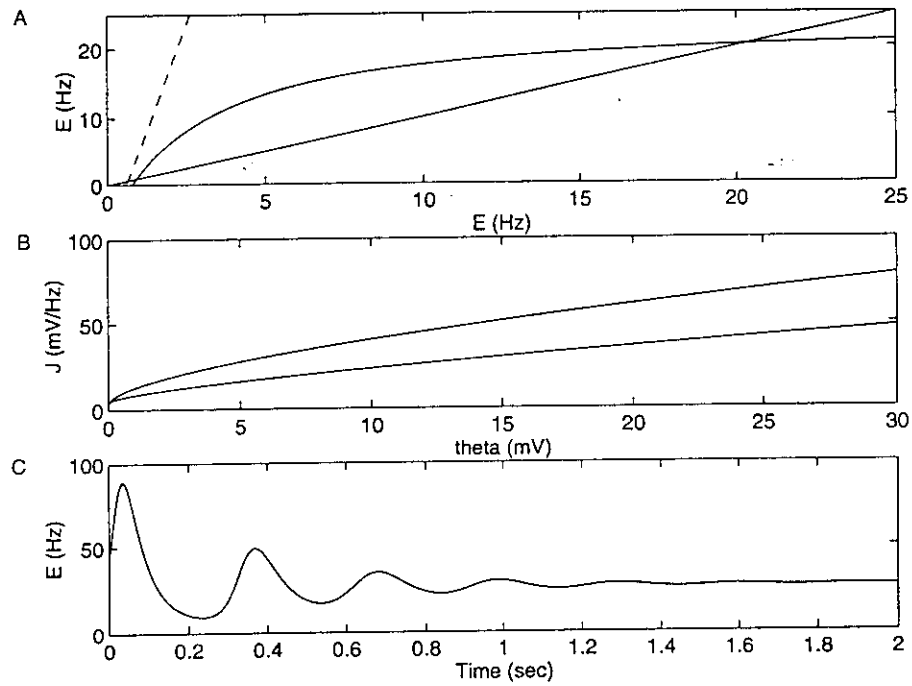

Figure 2: Solution of Eqs. 12 for the network of one excitatory population with homogeneous connections. (A): Graphical solution of the fixed point equation (13). The response function had a linear-threshold shape (dashed line) with the threshold θ and slope β. The fixed point solution is given by the intersection of the two solid lines. (B) Phase diagram of the system in the space of θ and J. (C) The solution of the dynamic equations (12). Parameters in (A) and (C): $\theta = 15$ mV; $\beta = 0.5$ mV^{-1}Hz $J = 60$ mV*Hz^{-1}; $U = 0.5$; $\tau_{rec} = 800msec$; $\tau = 30msec$.

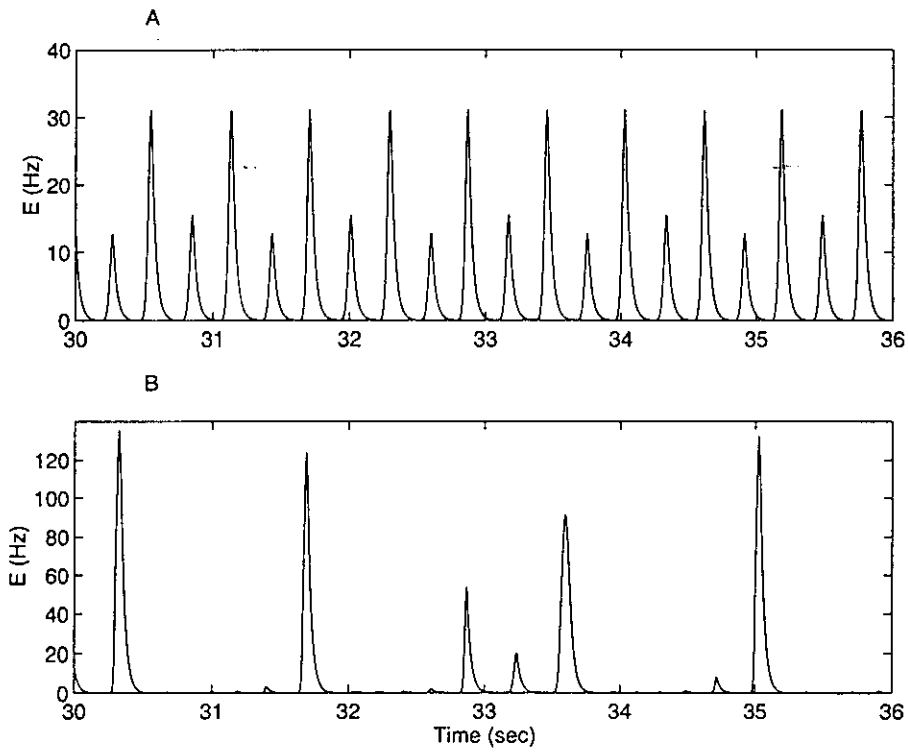

Figure 3: Solutions of Eqs. 11 for the network of two populations with homogeneous connections. (A): Population activity $E(t)$ for the parameters $I^e = 17$ mV; $I^i = 15$ mV; $J_{ee} = 50$ mV*Hz^{-1}; $J_{ei} = 40$; $J_{ie} = 70$; $J_{ii} = 19.5$; U =0.5 (ee and ei); $U = 0.05$ (ie); 0.03 (ii); $\tau_{rec} =$ 800 msec (ee and ei); 600 msec (ie); 850 msec(ii); $\tau_{facil} = 1000$ msec (ie); 400 msec (ii); $\tau_e =$ 30 msec; $\tau_i = 40$ msec. (B): The same as in A but with $J_{ii} = 0$. The gain functions for both populations have the same form as in Fig. 2.

5 Conclusion

We presented the derivation of self-consistent mean-field equations for the dynamic behavior of large neural networks with arbitrary architecture of external inputs and internal interactions. The formalism was illustrated by considering two simple examples of networks consisting of one and two uniform populations of neurons. The purely excitatory network was shown to always possess a fixed point solution which can have arbitrary small firing rates. Adding an inhibitory population greatly increases the repertoire of behaviors, including the irregular sequence of population bursts of various amplitudes. Synaptic dynamics could therefore be an important factor in generating different states of cortical activity as reflected by EEG recordings.

References

[1] Amit, D. J. & Tsodyks, M. Quantitative study of attractor neural network retrieving at low spike rates I: Substrate-spikes, rates and neuronal gain. *Network*, **2**, 259-274 (1991).

[2] Ginsburg, I. & Sompolinsky, H. Theory of correlations in stochastic neural networks. *Phys. Rev. E* **50**, 3171-3191 (1994).

[3] Markram, H. & Tsodyks, M. Redistribution of synaptic efficacy between pyramidal neurons. *Nature*, **382**, 807-810 (1996).

[4] Markram, H., Tsodyks, M. & Wang, Y. Differential signaling via the same axon of neocortical pyramidal neurons. *PNAS*, in press.

[5] Softky, W.R. & Koch, C. The higly irregular firing of cortical cells isinconsistent with temporal integration of random EPSPs. J. Neurosci. **13**, 334-350 (1993).

[6] Tsodyks, M. V. & Markram, H. The neural code between neocortical pyramidal neurons depends on neurotransmitter release probability. *PNAS* **94**, 719-723 (1997).

[7] Wilson, H. R. & Cowan, J. D. Excitatory and inhibitory interactions in localized populations of model neurons. *Biophys. Journ* **12**, 1-24 (1972).

Lecture 4: Synchrony Generation in Recurrent Networks with Frequency-Dependent Synapses

Misha Tsodyks

Department of Neurobiology, Weizmann Institute of Science, Rehovot 76100, Israel.

1 Summary

Throughout the brain, groups of neurons have been found to fire synchronously on the time scale of a few milliseconds. This near coincident firing of neurons could enable fast processing of sensory stimuli and/or regulate synaptic plasticity. The mechanisms of generating this form of synchrony are not known. In this lecture we discuss the possibility that near coincident firing of groups of neurons could result from population dynamics of interconnected networks, provided the connections between excitatory neurons exhibit synaptic depression. In our simulations, we demonstrate that these networks can exhibit a special regime of activity with sharp population bursts intermittent with the long periods of asynchronous firing. Before and during the bursts, neurons in the network tend to fire in the specific temporal order which depends on the neuron's spontaneous firing rates. Neurons with low rates are the ones firing the first and are responsible for generating the population bursts. The network can also generate population bursts in response to external excitatory inputs. This response is facilitated if neurons with low spontaneous rates are specifically targeted.

2 Introduction

While increased firing rate of a single neuron is the clearest signature of its participation in a particular processing, growing evidence indicates that temporal coherence in the activity of groups of neurons may be an important component of the neuronal code. Indeed, throughout the brain, the spiking activity of groups of cells found to exhibit various patterns of synchrony, during both spontaneous activity and under sensory stimulation (Murphy et al., 1985; Gray et al., 1989; Vaadia and Aertsen, 1992; Sillito et al., 1994; Riehle et al., 1997; Steriade and Contreras, 1998). Synchrony could allow the information about external stimuli to be coded in the temporal relation between the spiking of different neurons (Abeles, 1991; Hopfield, 1995) or provide the basis for binding different features belonging to the same object (Singer and Gray, 1995).

The mechanisms of inducing a synchronous firing in groups of cells are not yet directly accessible to experimental study. A pair of neurons could synchronize by means of either direct synaptic connection, or a common input, which in turn could be mediated by feedforward connections from lower areas, feedback connections from higher areas or recurrent connections originating in the same brain area where the neurons are located. Different mechanisms may be responsible for synchronization on different time scales. Anatomical evidence indicates that most of the synaptic contacts a cortical cell receives are in fact originating in the cells which are located in the same cortical area (Ahmed et al., 1994). It is therefore reasonable to assume that much of the observed synchronization is generated locally as a consequence of the population dynamics. Synchrony generation by networks of interconnected neurons was a subject of many theoretical and numerical studies. It is easy to construct a network in which a firing of individual neurons is perfectly *locked* to each other (Mirollo and Strogatz, 1990). On the other extreme, the network could be in the regime of *asynchronous* activity with independent firing of individual neurons (Abbott and van Vreeswijk, 1993). In this state, a neuron is adequately described by its firing rate as timing of individual spikes are not important. An intermediate regime of *synchronized*

chaotic activity was obtained in (Hansel and Sompolinsky, 1996), where only a fraction, albeit a large one, of spikes for a pair of neurons were synchronized on the time scale of few milliseconds.

Sharp synchronization between the spiking activity of pairs of neurons was reported in several studies (Murphy et al., 1985; Vaadia and Aertsen, 1992; Riehle et al., 1997). In none of these studies, however, full synchronization was observed, rather a small fraction of spikes were tightly locked, while the rest of the spikes were at most loosely correlated. This may suggest that cortical networks can operate in a regime in which asynchronous activity, well described by firing rates, is intermittent with sharp synchronization on the time scale of single spikes. In this lecture we demonstrate that such an intermittent regime of activity can be observed in the network behavior if one takes into account the nonlinear properties of synaptic transmission between the neurons.

3 Model

We simulated an interconnected network of 400 excitatory neurons and 100 inhibitory neurons. No specific architecture was assumed, rather the neurons were connected at random with a probability of a contact between a pair of neurons taken to be 10% in according with anatomical data (Abeles, 1991). Neurons were modeled as leaky integrate-and-fire units widely used in this kind of simulations (Tuckwell, 1988). Each unit is described by its voltage membrane potential which evolves according to a circuit equation

$$\tau \frac{dV}{dt} = -V + R_{in}(I_{syn} + I_{ff}), \tag{1}$$

where τ denotes the membrane time constant of a neuron, I_{syn} represents a synaptic current mediated by recurrent connections and I_{ff} stands for a feed-forward input current provided by the lower brain areas. The membrane potential V is measured relative to a resting level for a given neuron. Each time the membrane potential of a neuron reaches threshold ($15mV$ used in the simulations shown below), a spike is emitted and the voltage is instantaneously put to a reset value ($13.5mV$). For simplicity, I_{ff} is modeled as a fixed analog value different for different neurons. We assume that external current is distributed uniformly across the network, such that the distribution of $R_{in}I_{ff}$ is centered at the threshold level and has a std of $0.025mV$. This guarantees that the firing rates of the neurons are distributed between approximately $1Hz$ and $20Hz$. In most of the simulations, we did not include noise in the input to the neurons.

Synaptic current I_{syn}, on the other hand, is modeled as a sum of postsynaptic currents (PSCs) from all of the other neurons in the network which have connections targeting the given neuron (i):

$$I_{syn}(i) = \sum_j A_{ij} y_{ij}(t). \tag{2}$$

To calculate the synaptic current, we use the phenomenological model of dynamic synapses presented in the previous lectures. Briefly, A_{ij} is a parameter describing the *absolute* strength of synaptic connection between neurons j (presynaptic neuron) and i (postsynaptic neuron).

The *effective* synaptic strength is determined by the factor y_{ij} which describes the contribution to a synaptic current of neuron i due to PSCs from a neuron j. It evolves according to the system of kinetic equations:

$$\begin{aligned} \frac{dx}{dt} &= \frac{z}{\tau_{rec}} - ux\delta(t - t_{sp}) \\ \frac{dy}{dt} &= -\frac{y}{\tau_I} + ux\delta(t - t_{sp}) \\ \frac{dz}{dt} &= \frac{y}{\tau_I} - \frac{z}{\tau_{rec}} \end{aligned} \tag{3}$$

where x, y and z are the fractions of synaptic resources in the recovered, active and inactive states respectively; t_{sp} denotes a timing of pre-synaptic spikes; τ_I is the decay constant of PSCs and τ_{rec} is the recovery time from synaptic depression. These equation describe the utilization of synaptic resources by each presynaptic spike (fraction u of the available resources x is utilized by each presynaptic spike). A running variable u_{ij} describes the effective utilization of the synaptic resources in the synapses, which is analogous to probability of release in the quantal model (Markram et al., 1998). In facilitating synapses, it is increased with each presynaptic spikes and returns to the baseline value with a time constant of τ_{facil}:

$$\frac{du}{dt} = -\frac{u}{\tau_{facil}} + U(1 - u)\delta(t - t_{sp}). \tag{4}$$

where parameter U determines the increase in the value of u with each spike. If $\tau_{facil} \to 0$, facilitation is not exhibited and $u \equiv U$, as is the case with depressing synapses between excitatory pyramidal neurons (Tsodyks and Markram, 1997).

The synaptic parameters were assigned in a random fashion: for each type of the connections, the average values of the parameters were specified and then for each connection a parameter was chosen from the Gaussian distribution with the standard deviation taken as half of the average value. The average values of parameters for each type of the connection used in the simulations were taken from our studies of cortical synapses: $Aee = 1.8mV$; $Aei = 5.4mV$; $Aie = 7.2mV$; $Aii = 7.2mV$; $Uee = 0.5$; $Uei = 0.5$; $Uie = 0.04$; $Uii = 0.04$; $\tau_{rec}ee = \tau_{rec}ei = 800msec$; $\tau_{rec}ie = \tau_{rec}ii = 100msec$; $\tau_{facil}ie = \tau_{facil}ii = 1000msec$; $\tau_I = 3msec$.

4 Results of Simulations

4.1 Network dynamics

An epoch of network simulations is illustrated in Fig. 1. The plot of the population activity indicates that the network dynamics exhibit long intervals of almost asynchronous activity intermittent with sharp *population bursts* (PB; see Fig. 1B). With the choice of parameters given above, the network generates about 1 population burst per second. The duration of the PB is less then $15msec$, with most of the spikes emitted within $5msec$ around the peak of the burst. During the PB, most of the neurons fire 1 to 3 spikes in a rapid succession.

4.2 Mechanisms of population burst initiation

The presence of the PBs is an indication that the network operates in the regime in which asynchronous activity cannot last indefinitely due to accumulated instability caused by recurrent excitation. Indeed, since the synapses between excitatory neurons are depressing, the average effective strength of recurrent excitation is quickly decreases during the PB and slowly recovers between the consecutive PBs (Fig. 1C). The instability develops when excitation reaches a certain threshold value. The crucial role of synaptic depression of recurrent excitatory connections in generating this network behavior was confirmed by control simulations in which nonlinearity was eliminated in all other of connections, which resulted in a qualitatively similar network activity. We also checked that increasing the absolute strength (A) of recurrent excitatory connections leads to a higher frequency of PBs.

Since synaptic depression is responsible for PBs, it is reasonable to assume that the neurons with the lower firing rates should play a special role in their generation. This is because the effective strength of a depressing synapse is decreasing with the firing rate of the presynaptic neuron. To clarify this issue, we ordered the excitatory neurons according to the their average firing rates (Fig. 2A) over the interval of $20sec$. We were then selectively eliminating groups of 30 excitatory neurons, ranked according to their firing rates, and counted the number of remaining bursts in an interval of $20sec$ after the start of the simulations. As shown in Fig. 2B, the bursts disappear completely if the group of neurons with the firing rates from $1.3Hz$ to $2.5Hz$ is eliminated (Fig. 2B). One can explain this result by the fact that these neurons, while having a low firing rate and therefore effectively strong excitatory synapses, are at the same time close enough to threshold to serve as a driving force for the avalanche of the firing activity leading to a PB.

4.3 Population response to external stimulation

Spontaneous PBs can only be observed if the connections between excitatory neurons are strong enough. However, even if connections are weak, the network can still generate the bursts in response to an external stimulation. To demonstrate this possibility, we uniformly reduced the absolute strength of all the synapses in the network until the PBs disappeared. We then studied the response of the network to sharp input pulses of various amplitudes with a frequency of $1Hz$, targeting groups of 30 neurons. In Fig. 2C we plotted the minimal amplitude of the pulses needed to evoke a PB in the network, for different choices of the targeted group. As the firing rate of targeted neurons increases, the intensity of the pulse required for response PB decreases gradually, reaching the minimum for about the same group of neurons which are mostly responsible for spontaneous bursts generation (compare Figs. 2B,C). With the subsequent increase in the rate of targeted neurons, the bursts are evoked at sharply higher input intensity, until no bursts can be evoked at any input intensity when the neurons targeted have rates of more than $5Hz$. The network can therefore effectively differentiate between the external excitatory pulses targeting the groups of neurons with different spontaneous firing rates.

4.4 Temporal relationship between neuronal firing

The simulation results indicate that the network exhibits qualitatively different activity patterns during and between the PBs. To illustrate this difference, we computed the cross-correlation functions (CCF) between the firing of different pairs of neurons, over the period of 1000 seconds. In Fig. 3 we show an example of CCF for two neurons having the firing rates of close to $10Hz$. A sharp peak at zero time difference for the CCF is a direct result of the PBs during which both of the neurons fire within a short time interval. If one excludes the spikes emitted during the PBs, the resulting CCF does not exhibit any substantial peaks, indicating that between the bursts the firing of neurons remains essentially asynchronous. The area under the central peak in the CCF equals 10 percent of the overall number of spikes emitted by each of the neurons, which corresponds to the relative number of spikes emitted during the PBs . In Fig. 3B, we show another pair, this time with one of the neurons having a low firing rate of about $2Hz$. The small negative bias of $4msec$ in the CCF can be detected, indicating that the neuron with the lower firing rate systematically fired before the neuron with high rate. This is consistent with the previous observation that the neurons with low firing rate play a crucial role in generating the PBs. Finally, Fig. 3C illustrates a pair of neurons with low rates, which exhibit a CCF with two sharp peaks at both positive and negative time difference.

The shape of CCFs indicates that there exists a statistically reproducible timing relation between the firing of different neurons during a PB. To illustrate this relation, we computed, for each neuron in the network, the CCF between the neuron's spike train and the peaks of the population bursts, and marked the time at which CCF was at its maximum (Fig. 4). As seen by comparison between Figs. 2B and 4, the neurons which are responsible for PBs generation, systematically fire in the advanced phase of the PB.

5 Conclusion

The simulations presented in this lecture demonstrate that networks of neurons interconnected with dynamic synapses can generate a special regime of activity with population bursts intermittent with the long periods of asynchronous activity. As a result of the PBs, the neurons can exhibit synchronous firing characterized by a small fraction of spikes emitted within a time window of few milliseconds. The network can also produce PBs in response to external excitatory pulses. In this case, the response of the network is facilitated if the pulses target the subpopulation of neurons with low spontaneous firing rates. Synaptic depression between excitatory neurons plays a crucial role in generating this network behavior. We also emphasize that synchronization between neurons on the time scale of few milliseconds can be achieved in randomly connected networks, without any specific structures such as synfire chains.

The conclusion of the analysis could be tested experimentally by recordings from multiple neurons in the same cortical area. The results of the simulations predict that groups of cells can generate tightly synchronous spikes on the scale of few milliseconds, intermittent with the long periods with no synchronization on this scale. This effect could be observed during either spontaneous firing or during the response to sensory stimulation. There should also

exist a systematic temporal relation between the timing of spikes in pairs of neurons in relation to their average firing rate. In particular, the spikes of neurons with low firing rates should precede the spikes of neurons with higher rates.

One could speculate that PBs observed in simulations could have a functional significance for cortical networks. Since long-term regulation of synaptic transmission was shown to be sensitive to relative timing of spikes between pre- and post-synaptic neurons (Markram et al., 1997), spontaneous PBs could influence the shaping of local functional connectivity in the cortex. The PBs evoked by the external input could provide the cortex with the ability for a fast processing of the sensory stimuli, in accordance with recent psychophysical results (Thorpe et al., 1996).

6 Figures

Figure 1. Network dynamics. (A) Spike trains of every 5th neuron in a time window of $3.5sec$. For each neuron, a dot is put at each time the neuron emitted an action potential. (B) Population activity, computed as an overall number of action potentials emitted during consecutive bins of $1msec$. In the inset, the network activity during the time window of $40msec$ around the population burst is shown. (C) The plot of the parameter x, describing the running effective strength of depressing synapses), averaged over all connections between excitatory neurons.

Figure 2. Mechanism of population burst initiation. (A) Firing rates of the excitatory neurons in the network, in the increasing order, computed over the time interval of $20sec$. (B) The number of population burst over the same interval, which are observed in simulations with a group of 30 neurons, starting from the neuron indicated on the horizontal axis, are taken out of the network. (C) The network with the absolute strength (A) of all connections reduced by 1/3 of the original values, resulting in the disappearance of spontaneous population bursts. For each group of neurons, the input pulse of the duration of $5msec$ is applied with the frequency of $1Hz$. The minimal amplitude of the pulse (in mVs) which is required to reliably evoke a population burst is plotted for each group of 30 targeted neurons.

Figure 3. Typical examples of crosscorrelation functions for 3 pairs of neurons. Solid line - crosscorrelation function computed over the period of $1000sec$ of activity; dashed line - crosscorrelation function computed over the the same time period but subtracting the spikes emitted during the population bursts of the network. (A) Two neurons with similar rates in the middle of the rate distribution ($10Hz$ and $12Hz$). (B) A pair of neurons with the rates $1.7Hz$ and $12Hz$. (C) A pair of neurons with the low rates of $2.6Hz$ and $1Hz$.

Figure 4. Temporal relationship between the firing of excitatory neurons and the population bursts. For each neuron, the crosscorrelation function between its spike train and the times of the maximums of population bursts is computed and the time difference at which the crosscorrelation function is at its maximum is plotted.

References

Abbott, L. F. and van Vreeswijk, C. (1993). Asynchronous states in networks of pulse-coupled oscillators. *Phys. Rev. E*, 48:1483–1490.

Abeles, M. (1991). *Corticonics*. Cambridge University Press, New York.

Ahmed, B., Anderson, J., Douglas, R., Martin, K., and Nelson, J. (1994). Polyneural innervation of spiny stellate neurons in cat visual cortex. *J. Comp. Neurol.*, 341:39–49.

Gray, C. M., Konig, P., Engel, A. K., and Singer, W. (1989). Oscillatory responses in visual cortex exhibit intercolumnar synchronization which reflects global stimulus properties. *Nature*, 338:334–337.

Hansel, D. and Sompolinsky, H. (1996). Chaos and synchrony in a model of a hypercolumn in visual cortex. *J. Comp. Neurosci.*, 3:7–34.

Hopfield, J. J. (1995). Pattern recognition computation using action potential timing for stimulus representation. *Nature*, 376:33–36.

Markram, H., Lübke, J., Frotscher, M., and Sakmann, B. (1997). Regulation of synaptic efficacy by coincidence of postsynaptic APs and EPSPs. *Science*, 275:213–215.

Markram, H., Wang, Y., and Tsodyks, M. (1998). Differential signaling via the same axon from neocortical layer 5 pyramidal neurons. *PNAS*, 95:5323–5328.

Mirollo, R. E. and Strogatz, S. H. (1990). Synchronization of pulse-coupled biological oscillators. *SIAM J. Appl. Math.*, 6:1645–1657.

Murphy, J. T., Kwan, H. C., and Wong, Y. C. (1985). Cross-correlation studies in primate motor cortex: Synaptic interaction and shared input. *Can. J. Neurol. Sci.*, 12:11–23.

Riehle, A., Grün, S., Diesman, M., and Aertsen, A. (1997). Spike synchronization and rate modulation differentially involved in motor cortical function. *Science*, 278:1950–1953.

Sillito, A. M., Jones, H. E., Gerstein, G. L., and West, D. C. (1994). Feature-linked synchronization of thalamic relay cell firing induced by feedback from the visual cortex. *Nature*, 369:479–482.

Singer, W. and Gray, C. M. (1995). Visual feature integration and the temporal correlation hypothesis. *Annual Review of Neuroscience.*, 18:555–586.

Steriade, M. and Contreras, D. (1998). Spike-wave complexes and fast components of cortically generated seizures. i. role of neocortex and thalamus. *J. Neurophysiol.*, 80:1439–1455.

Thorpe, S., Fize, D., and Marlot, C. (1996). Speed of processing in the human visual system. *Nature*, 381:520–522.

Tsodyks, M. and Markram, H. (1997). The neural code between neocortical pyramidal neurons depends on neurotransmitter release probability. *PNAS*, 94:719–723.

Tuckwell, H. C. (1988). *Introduction to theoretical neurobiology.* Cambridge University Press, New York.

Vaadia, E. and Aertsen, A. (1992). Coding and computation in the cortex: single-neuron activity and cooperative phenomena. In Aertsen, A. and Braitenberg, V., editors, *Information Processing in the Cortex*, pages 81–121. Springer-Verlag.

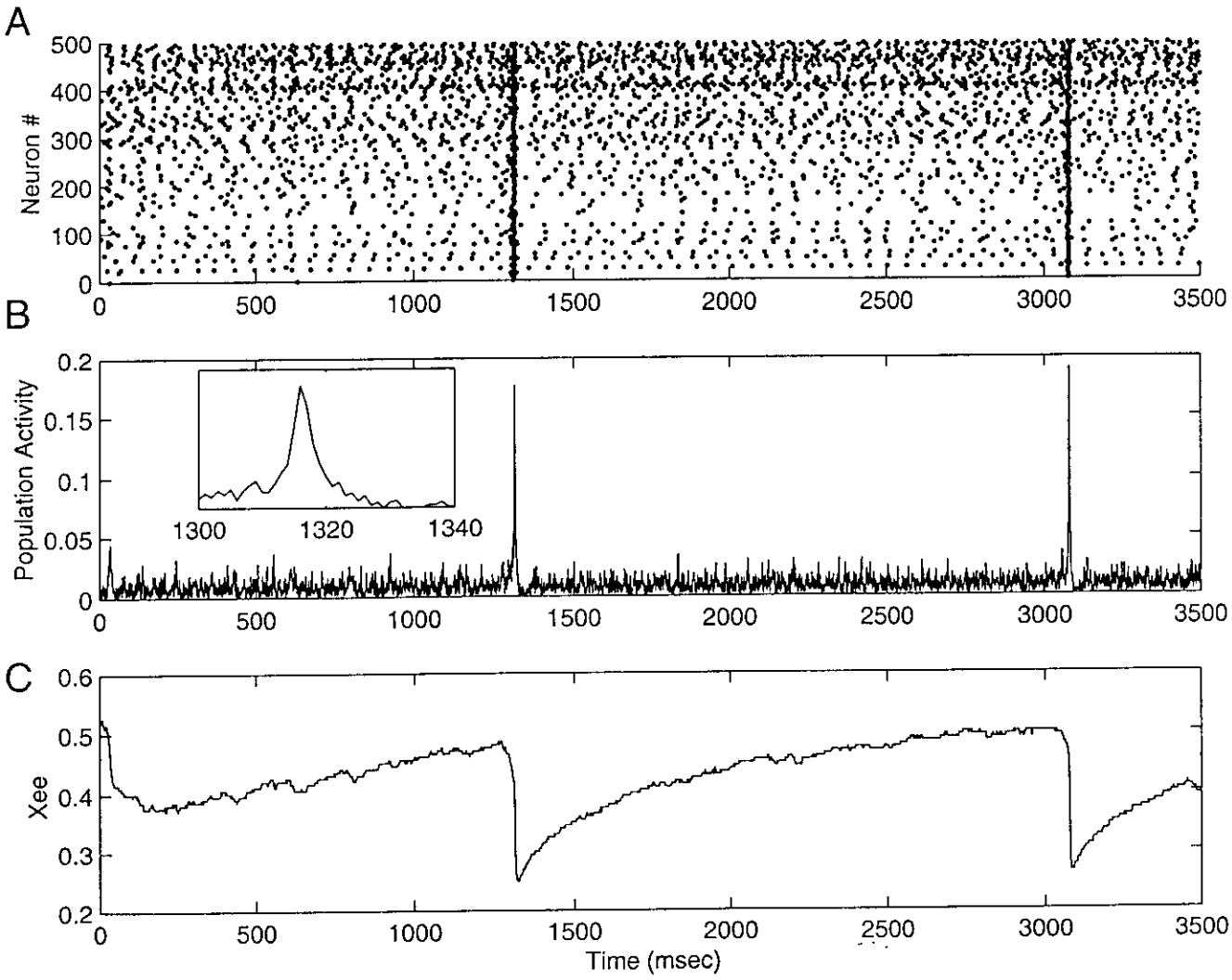
A
Neuron #
500
400
300
200
100
0
0
500
1000
1500
2000
2500
3000
3500
B
Population Activity
0.2
0.15
0.1
0.05
0
1300
1320
1340
C
Xee
0.6
0.5
0.4
0.3
0.2
Time (msec)

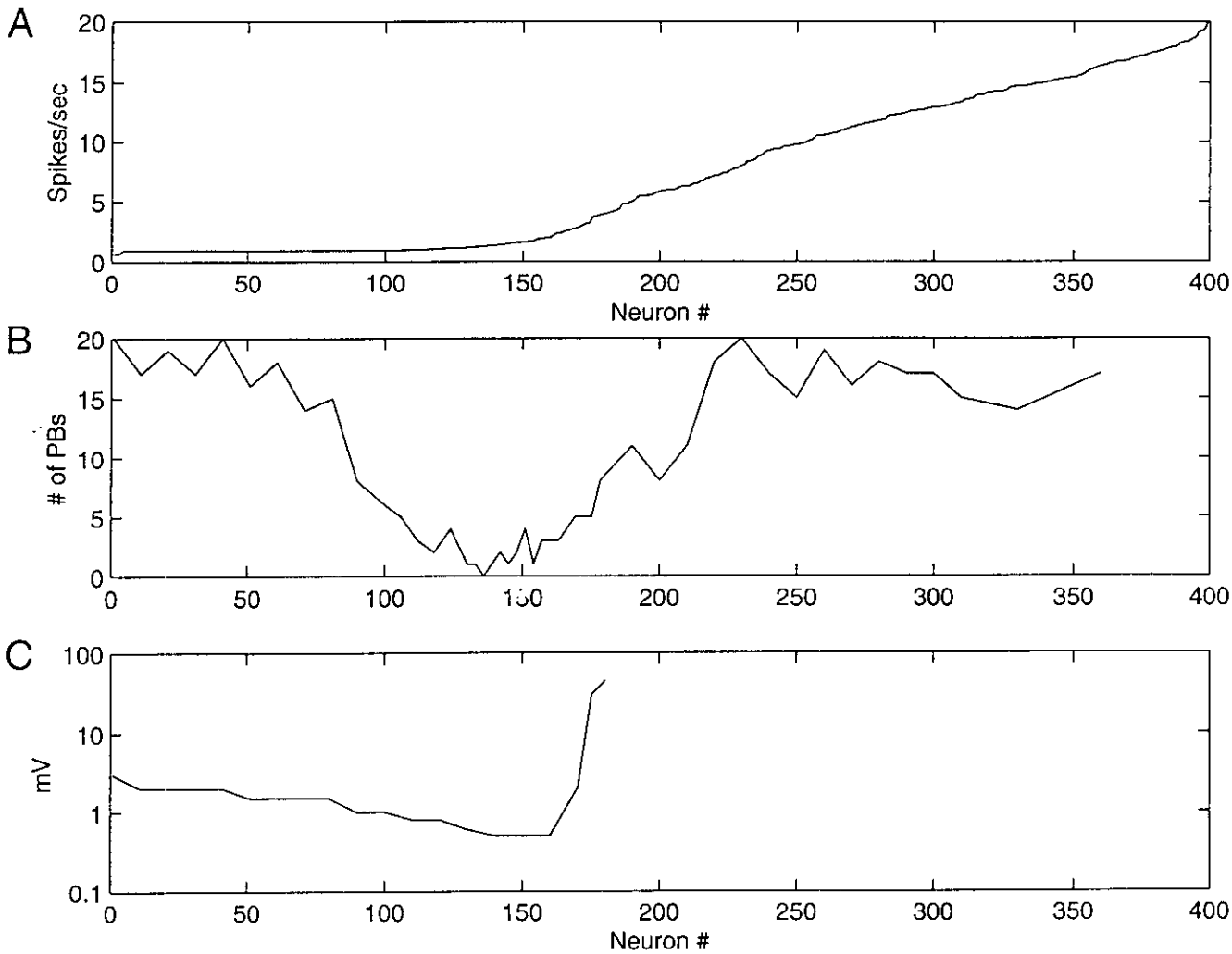
A
Spikes/sec
0
5
10
15
20
0
50
100
150
200
250
300
350
400
Neuron #
B
# of PBs
0
5
10
15
20
0
50
100
150
200
250
300
350
400
C
mV
0.1
1
10
100
0
50
100
150
200
250
300
350
400
Neuron #

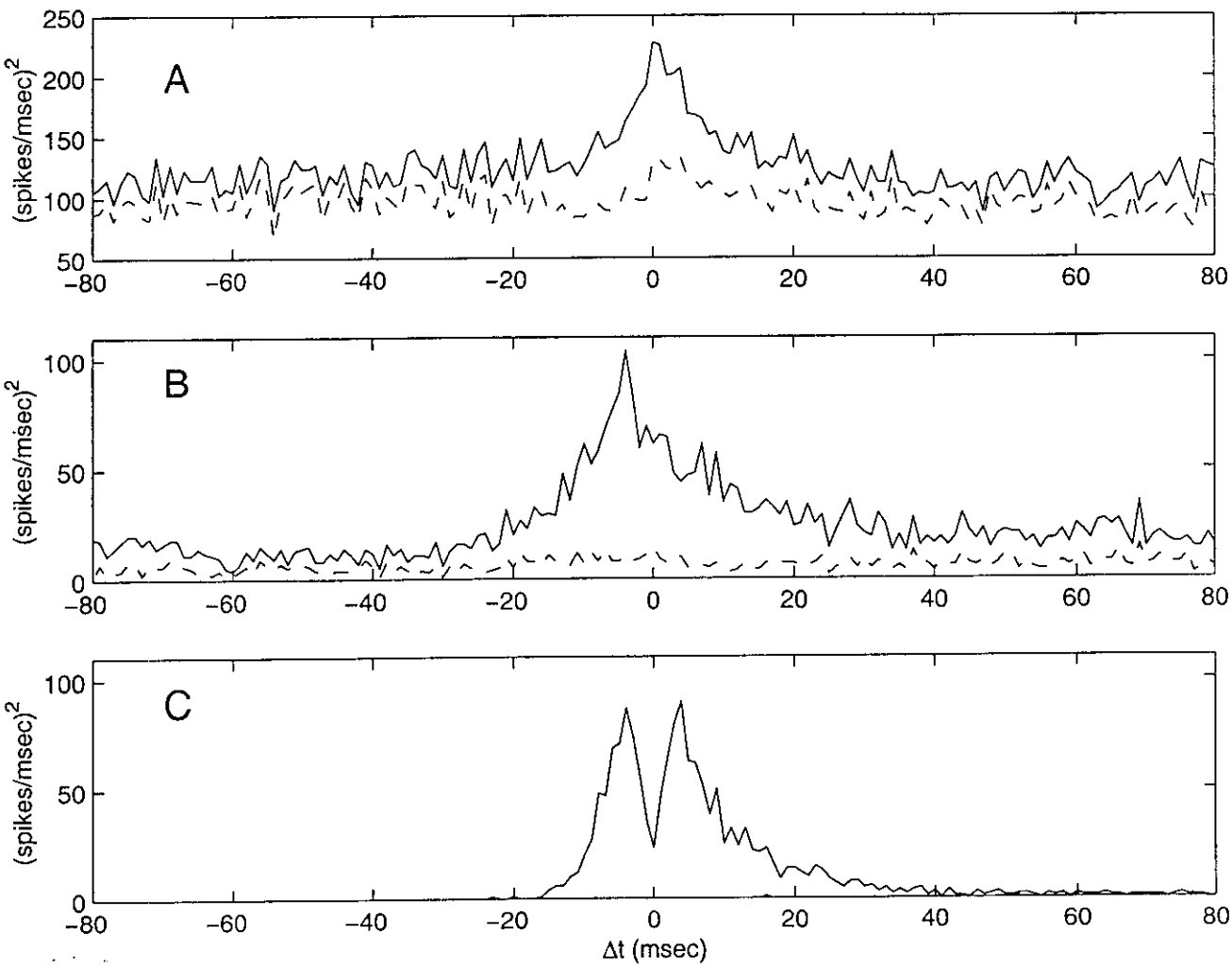
A
B
C
(spikes/msec)^2
250
200
150
100
50
0
−80
−60
−40
−20
0
20
40
60
80
Δt (msec)

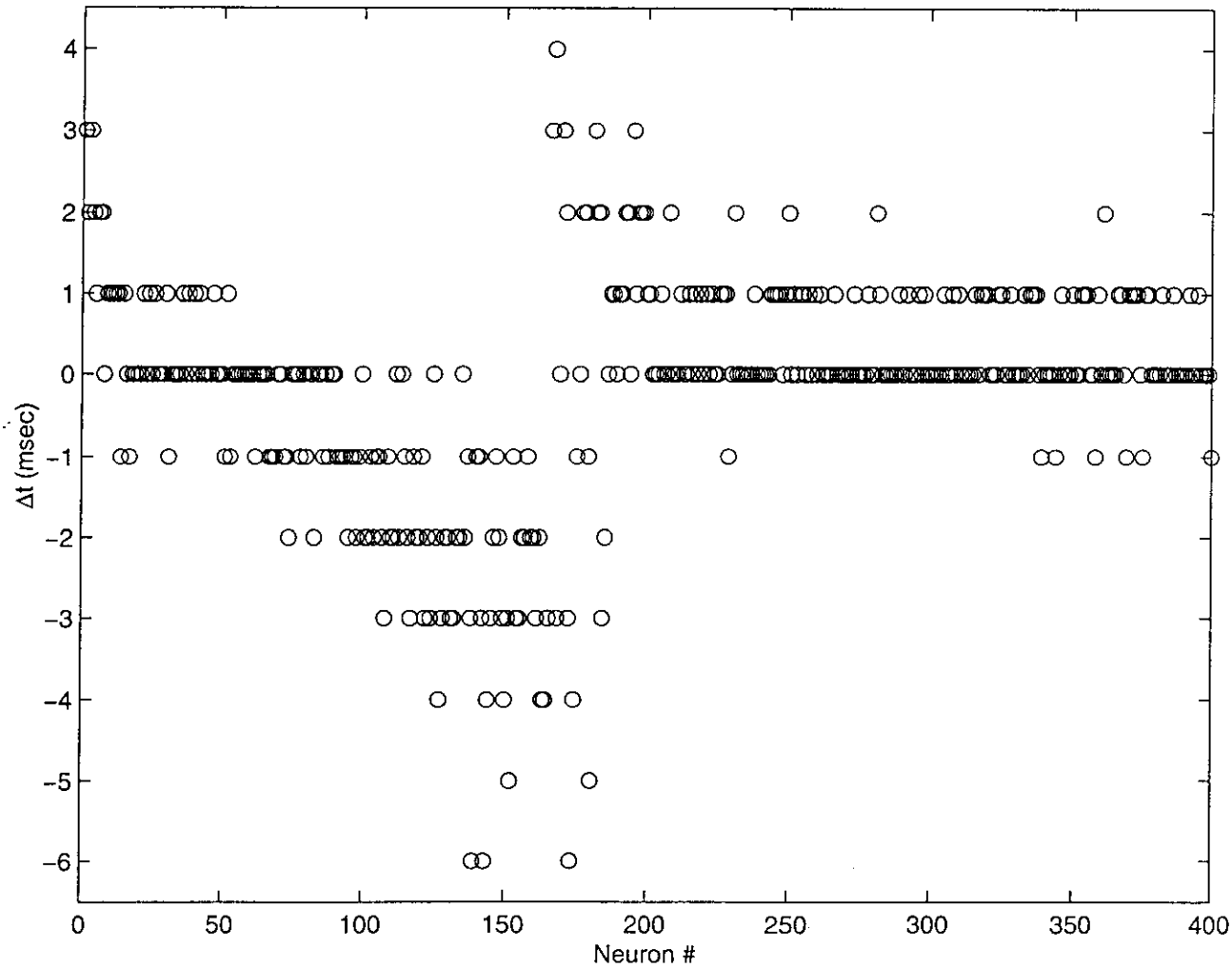
4
3
2
1
0
−1
−2
−3
−4
−5
−6
Δt (msec)
0
50
100
150
200
250
300
350
400
Neuron #